



ELSEVIER



CrossMark

Available online at [www.sciencedirect.com](http://www.sciencedirect.com)**ScienceDirect**

Physics Procedia 66 (2015) 514 – 519

Physics

**Procedia**

C 23rd Conference on Application of Accelerators in Research and Industry, CAARI 2014

## A MAPS Based Micro-Vertex Detector for the STAR Experiment

Joachim Schambach<sup>a,\*</sup>, Eric Anderssen<sup>b</sup>, Giacomo Contin<sup>b</sup>, Leo Greiner<sup>b</sup>, Joe Silber<sup>b</sup>,  
Thorsten Stezelberger<sup>b</sup>, Xiangming Sun<sup>c</sup>, Michal Szelezniak<sup>d</sup>, Flemming Videbaek<sup>e</sup>,  
Chinh Vu<sup>b</sup>, Howard Wieman<sup>b</sup>, Sam Woodmansee<sup>b</sup>

<sup>a</sup>University of Texas, 1 University Station, Austin, TX 78712, USA

<sup>b</sup>Lawrence Berkeley National Laboratory, Berkeley, CA 94720

<sup>c</sup>Central China Normal University (CCNU), Wuhan, China

<sup>d</sup>Institut Pluridisciplinaire Hubert Curien (IPHC), Strasbourg, France

<sup>e</sup>Brookhaven National Laboratory, Upton, NY 11973, USA

### Abstract

For the 2014 heavy ion run of RHIC a new micro-vertex detector called the Heavy Flavor Tracker (HFT) was installed in the STAR experiment. The HFT consists of three detector subsystems with various silicon technologies arranged in 4 approximately concentric cylinders close to the STAR interaction point designed to improve the STAR detector's vertex resolution and extend its measurement capabilities in the heavy flavor domain. The two innermost HFT layers are placed at radii of 2.8 cm and 8 cm from the beam line. These layers are constructed with 400 high resolution sensors based on CMOS Monolithic Active Pixel Sensor (MAPS) technology arranged in 10-sensor ladders mounted on 10 thin carbon fiber sectors to cover a total silicon area of 0.16 m<sup>2</sup>. Each sensor of this PiXeL ("PXL") sub-detector combines a pixel array of 928 rows and 960 columns with a 20.7 μm pixel pitch together with front-end electronics and zero-suppression circuitry in one silicon die providing a sensitive area of ~3.8 cm<sup>2</sup>. This sensor architecture features 185.6 μs readout time and 170 mW/cm<sup>2</sup> power dissipation. This low power dissipation allows the PXL detector to be air-cooled, and with the sensors thinned down to 50 μm results in a global material budget of only 0.4% radiation length per layer. A novel mechanical approach to detector insertion allows us to effectively install and integrate the PXL sub-detector within a 12 hour period during an on-going multi-month data taking period. The detector requirements, architecture and design, as well as the performance after installation, are presented in this paper.

© 2015 The Authors. Published by Elsevier B.V. This is an open access article under the CC BY-NC-ND license

(<http://creativecommons.org/licenses/by-nc-nd/4.0/>).

Selection and peer-review under responsibility of the Organizing Committee of CAARI 2014

**Keywords:** Monolithic Active Pixel Sensor; Vertex Detector; Heavy Flavor; Silicon Detector

\* Corresponding author. Tel.: +1-512-471-1303; fax: +1-512-471-9637.

E-mail address: [jschamba@physics.utexas.edu](mailto:jschamba@physics.utexas.edu)

## 1. Introduction

One of the main goals of the STAR (“Solenoidal Tracker At RHIC”) experiment at the Relativistic Heavy Ion Collider (RHIC) at the Brookhaven National Laboratory is to study p+p, d+Au, and Au+Au collisions at several energies up to  $\sqrt{s} = 200$  GeV for Au+Au and up to  $\sqrt{s} = 510$  GeV for p+p collisions with the aim to reproduce and characterize the QCD phase transition between hadrons and partons (J. Adams et al., 2005). Heavy quark hadrons are suggested as a clean probe for studying the early dynamic evolution of the dense and hot medium created in these high-energy nuclear collisions. Most heavy quarks produced in these collisions end up as open heavy flavor particles. Until recently the rare production of heavy quarks and large combinatorial background in heavy ion collisions made the measurements of heavy flavor particles very difficult in the existing STAR sub-detector systems. Before the 2014 run of RHIC a new silicon based micro-vertex detector called the “Heavy Flavor Tracker” (HFT) was installed in STAR, which allows to measure decay vertices of open heavy flavor particles with very short ( $c\tau \sim 100 \mu\text{m}$ ) lifetimes (such as the  $D^0$  and  $D^*$  mesons and the  $\lambda_c$  baryon) by direct topological reconstruction.

## 2. Design

The main detector of the STAR experiment for charged particle track reconstruction is a Time Projection Chamber (TPC) inside a Solenoidal magnet (0.5 T), which covers  $\pm 1$  units of pseudo-rapidity around mid-rapidity and the full azimuth. It has a Distance of Closet Approach (DCA) pointing resolution of about 1 mm towards the interaction vertex. The decay length of open heavy flavor particles is very small; for example, the  $c\tau$  of  $D^0$  mesons is about 120  $\mu\text{m}$ . Therefore, one of the primary physics requirements for the HFT upgrade (D. Beavis et al., 2011) is to provide vertex pointing capability to resolve decay vertices displaced from the primary collision vertex by less than 150  $\mu\text{m}$ . The basic idea behind the HFT is to do tracking from the outside in with graded resolution. To achieve this goal, the HFT consists of 3 different silicon detector subsystems arranged in 4 concentric cylindrical layers around the primary vertex. The outmost detector subsystem is the Silicon Strip Detector (SSD), which consists of a double-sided silicon strip module with 95  $\mu\text{m}$  pitch at a radius of 22 cm from the beam line. It has a space point resolution of about 20  $\mu\text{m}$  in the  $r \times \phi$  direction and 740  $\mu\text{m}$  in the z (beam) direction. The next layer at 14 cm radius from the beam line is called the Intermediate Silicon Tracker (IST) and is constructed of single-sided double-metal silicon pad sensors with 600  $\mu\text{m} \times 6$  mm pitch, which achieves a space point resolution of 170  $\mu\text{m}$  in the  $r \times \phi$  direction and 1.8 mm in the z direction. The two innermost layers of the HFT at 2.8 cm and 8 cm from the beam line are called the Pixel detector (PXL) with the highest resolution ( $\sim 12 \mu\text{m}$ ) of the three HFT detector subsystems. The IST and SSD detectors’ aim is to guide charged particle tracks found in the outside TPC to the innermost PXL detector in a high hit density event.

The PXL subsystem consists of 10 trapezoidal carbon fiber sector tubes with four 10-sensor ladders mounted on each sector, 3 at the outer diameter (8 cm), and one at the inner diameter (2.8 cm). The sectors are assembled into two halves on mechanical supports with kinematic mounts that allow the insertion and retraction of the detector from one side of STAR in only about 12 hours, by pushing the halves along rails inside the support cylinder and locking them into kinematic mounts. The sensors are connected to aluminum conductor kapton flex cables that provide the signal path to electronics at the end of the flex cable containing the buffers and drivers for the sensor signals. The sensors are thinned to 50  $\mu\text{m}$ , resulting in a total radiation length  $X/X_0$  as small as 0.4% for the inner layer. A schematic view of the PXL detector is shown in Figure 1.

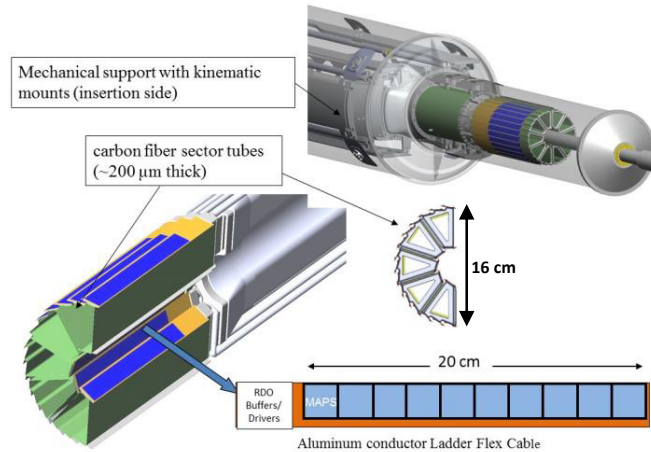


Fig. 1: A schematic view of the PXL sub-detector of the HFT

The PXL detector covers about the same phase space as the TPC, namely  $-1 \leq \eta \leq 1$  in pseudo-rapidity and full azimuth coverage. The sensors chosen for the PXL detector are based on state-of-the-art “Monolithic Active Pixel Sensor” (MAPS) technology, which uses a thin ( $15 \mu\text{m}$ ) epitaxial layer for charged particle detection with the readout circuitry integrated into a monolithic structure of a silicon chip. The sensors chosen for the PXL detector were designed by the PICSEL group of IPHC in Strasbourg, France (C. Hu-Guo et al., 2010; A. Dorokhov et al., 2010; A. Dorokhov et al., 2011; L. Greiner et al., 2011). This sensor uses pixels with a  $20.7 \mu\text{m}$  pitch arranged in a 928 (rows)  $\times$  960 (columns) array (a total of  $\sim 890\text{k}$  pixels per sensor) on a  $20.22 \text{ mm} \times 22.71 \text{ mm}$  silicon chip. The sensors are fabricated with a Hi-Resistivity epitaxial substrate chosen for improved Signal-to-Noise performance and radiation hardness. The frame readout time of the whole sensor array is  $185.6 \mu\text{s}$ , which is achieved by processing pixel columns in parallel, row by row. Each pixel includes amplification and correlated double sampling (CDS) circuitry, and each end of a column is equipped with a programmable threshold discriminator. After analog readout and signal digitization, the signals are passed through a zero-suppression system located below the pixel array on the same silicon chip, which delivers run-length encoded hit addresses for up to 9 hit clusters per row to one of two banks of on-chip memory for intermediate buffering (a “hit cluster” is a series of up to 4 consecutive pixels above threshold). Two memory banks of up to 1500 words are implemented in a Ping-Pong arrangement on the chip to allow simultaneous reading and writing. The data are finally read out bit-serially over two “Low-Voltage Differential Signaling” (LVDS) outputs per sensor, each running at 160MHz. The power dissipation of one of these sensors is only  $\sim 170 \text{ mW/cm}^2$ , which allows these sensors to be operated at room temperature with air-cooling. Configuration of the operational parameters as well as several test modes of the sensor are implemented over a “Joint Test Action Group” (JTAG) interface.

The readout electronics are divided into ten identical parallel systems following the mechanical segmentation of the PXL detector into sectors. At the end of each ladder and out of the low-mass region are readout buffers and cable drivers that send the binary zero-suppressed data over  $\sim 2 \text{ m}$  of low-mass twisted pair cable to the “Mass Termination Board” (MTB). The MTB provides additional buffering and drives the signals to the Readout (RDO) board; it also provides latch-up protected power supplies for the ladders. Each MTB services 4 ladders (one sector), i.e. there are 10 MTB’s in the PXL detector. The sensor data are then transmitted over  $\sim 13 \text{ m}$  of twisted-pair cable to an RDO board in the low radiation area of the STAR experimental hall. The “Field Programmable Gate Array” (FPGA) based RDO board receives the data, does trigger based hit selection, buffers, and formats the resulting data into event structures, and then sends it over 100 m optical fibers to one of ten fiber readout channels mounted in two PCs in the DAQ room. These DAQ PCs are connected to the rest of STAR DAQ for event building, where the PXL data are combined with the data from the other STAR detector subsystems providing data for the same event. The complete readout system for PXL consists of 10 RDO boards corresponding to the 10 PXL sectors and are mounted

in one 9U-size crate just outside the STAR detector. In addition to providing the readout of the PXL sensors and the interface to the STAR trigger and DAQ, the RDO boards also provide monitoring data to the STAR Slow Controls system and receive configuration data for the PXL sensors from a control PC in the counting house.

### 3. PXL Status and Performance

The goal of the PXL project is to deliver 2 full detector copies and 40 additional spare ladders to STAR. The full HFT system including all 3 subsystems was installed before the 2014 run. The PXL detector was inserted and cabled into the STAR TPC inner field cage and operational within a 2 day installation. At the time of installation all 400 sensors of the PXL system were working with less than 2000 bad pixels out of the more than 365 million total. A scan of noise rate versus discriminator threshold was performed and the thresholds were adjusted to give a fake hit rate of  $\sim 1.5 \cdot 10^{-6}$  for all sensors.

After installation, but before the 2014 RHIC run, cosmic ray data were taken for commissioning, alignment and efficiency studies. This period was also used to commission and integrate the PXL readout electronics with the existing STAR DAQ, Trigger, and Slow Controls systems. The efficiency of the PXL detector was obtained from these data by finding cosmic ray tracks with hits on 3 PXL sensors, and looking for hits on a fourth sensor at the position of the extrapolated straight line through these three hits. Although this study was done before the detector operational parameter optimization was complete, the average efficiency over all sensors was determined to be 97.2%. The same data were then used to align the different parts of the PXL detector by looking at the hit residuals compared to the track projections and adjusting the positions of the sensors in order to minimize these residuals. Gaussian fits to the residual (for the inner layer) after alignment are shown in Figure 2 resulting in a  $\sigma \leq 25 \mu\text{m}$ , which exceeds the design goals.

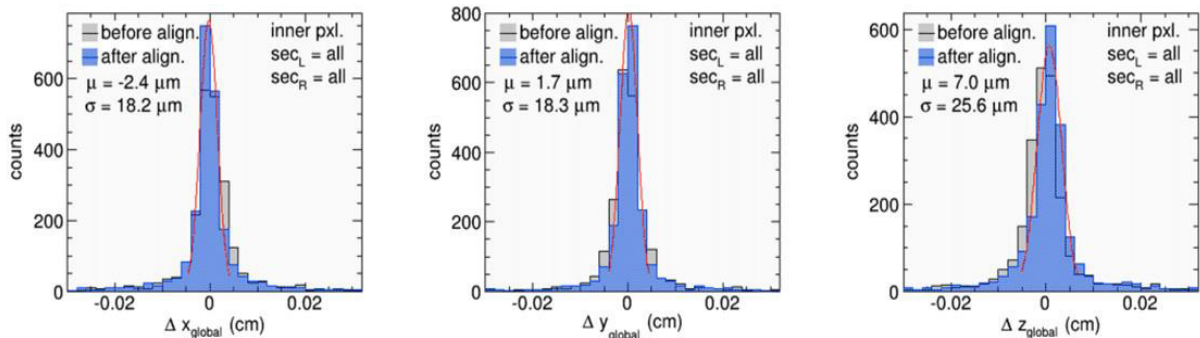


Fig. 2: PXL hit residuals of cosmic tracks before and after PXL sector alignment

The initial  $\sqrt{s} = 14.5$  GeV Au+Au run (Feb. 14 until Mar. 11) was used to optimize the sensor performance, but data was only collected in very few of the runs during this period. This short period was followed by the  $\sqrt{s} = 200$  GeV Au+Au run after March 15, and a total of 1.2B minimum bias events with PXL included were recorded in  $\sim 17$  weeks running. The PXL system was typically triggered at a rate of about 1 kHz, and at this rate the PXL detector produced data at a rate of about 120 MB/s with less than 5% dead time. Daily noise runs without beam collisions were recorded to reassess the sensor status, find hot or not working pixels, and to verify the noise level. Periodic threshold scans were performed to measure fake hit rate as a function of threshold and readjust the threshold settings.

After the survey and alignment corrections were done, the 200 GeV data were used to determine the pointing resolution to the collision point of the PXL detector. Figure 3 shows the DCA resolution for tracks found in the TPC, which have 1 hit in the IST and 1 hit in both layers of the PXL detector as a function of transverse momentum  $p_T$ . From these plots one can see that the design performance goal of  $60 \mu\text{m}$  for kaons with  $p_T = 750$  MeV/c was exceeded. In fact for  $p_T$  larger than 1.5 GeV/c the DCA resolution is better than  $30 \mu\text{m}$ .

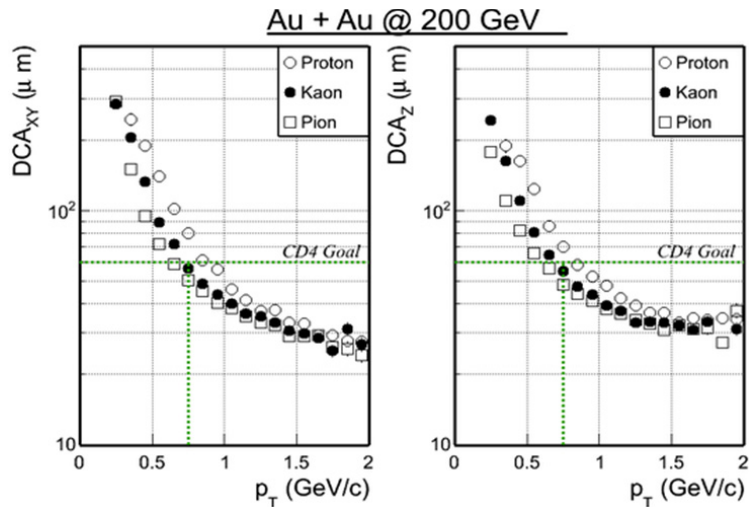


Fig. 3: DCA resolution for TPC tracks with 1 IST hit and hits in both layers of PXL vs. transverse momentum

As with any solid state detector, the PXL sensors are sensitive to radiation effects. First sensor damage was observed in the last week of the  $\sqrt{s} = 14.5$  GeV run after several beam loss events; damage continued to manifest itself in the  $\sqrt{s} = 200$  GeV run. The sensor damage appears to be radiation related possibly due to latch-up events in the thinned sensors and takes on many different forms: increased digital current, damaged or total loss of pixel columns, damaged configuration registers, loss of full or partial sub arrays, etc. Most of the damage occurred in sensors in the inner layer, but even in the outer layer some sensors were affected. A total of 14% of the PXL coverage in the inner layer and about 1% coverage in the outer layer were lost about one month into the 200 GeV Au+Au run. Several operational methods were developed early into the 200 GeV run and used for the rest of the run, which limited further damage to the sensors. For example, the digital voltage to the sensors was power cycled and the sensors reconfigured every 15 minutes; and most importantly, the threshold at which the digital power supplies to the sensors would latch up was reduced from initially 400 mA (allowing for large current excursions during radiation events) to 120 mA above the measured operating current on a ladder-by-ladder basis. After implementation of these operational methods, only two more sensors incurred additional radiation damage in the remaining 3 months of the 2014 run. We plan to implement these procedures from the beginning of the next RHIC run to limit damage to the PXL detector in the future. A test run with several production sensors at LBNL is planned to further investigate the cause of the observed damage.

#### 4. Outlook and Conclusions

State-of-the art MAPS sensors used for the PXL detector of the HFT were used for the first time in a collider experiment for a vertex detector. About 1.2 billion minimum bias Au+Au collision events at  $\sqrt{s} = 200$  GeV were recorded with the IST and PXL systems included and these data will enhance or enable heavy flavor measurements at STAR by allowing for reconstruction of displaced decay vertices very close to the interaction point. By the end of the 2014 run, all three detector subsystems of the HFT were commissioned and integrated into the STAR infrastructure and preliminary results for the DCA pointing resolution performance meets or exceeds the design goals. A second full PXL detector and additional spare ladders will be constructed by the summer 2014, and the damaged ladders of the initial PXL detector will be replaced. The second PXL detector will be installed in STAR for the 2015 RHIC run. Sensor damage related to the radiation field in STAR was observed, but appears to be significantly improved by using operational methods. MAPS as technology for vertex detectors in collider

experiments seems to be working well, and with the other detector systems in the HFT will greatly enhance our understanding of the quark state of matter created in heavy ion collisions at RHIC.

## Acknowledgements

This work was supported in part by the U. S. Department of Energy, Office of Science, Office of Nuclear Physics, Office of Heavy Ion Nuclear Physics under Award Number DE-FG02-94ER40845. We gratefully acknowledge the PICSEL group of IPHC Strasbourg (Marc Winter et al.) for the development of the PXL detector sensors.

## References

- J. Adams, et al., “Experimental and theoretical challenges in the search for the quark–gluon plasma: The STAR Collaboration's critical assessment of the evidence from RHIC collisions,” *Nucl. Phys. A*, vol. 757, pp. 102-183, Aug. 2005.
- D. Beavis et al., “The STAR Heavy Flavor Tracker Technical Design Report”, <https://drupal.star.bnl.gov/STAR/starnotes/public/sn0600>, 2011.
- C. Hu-Guo, et al., “First reticule size MAPS with digital output and integrated zero suppression for the EUDET-JRA1 beam telescope,” *Nucl. Instr. And Meth. A*, vol. 623, pp. 480-482, Nov. 2010.
- A. Dorokhov, G. Bertolone, J. Baudot, A.S. Brogna, C. Colledani, G. Claus, R. De Masi, M. Deveaux, G. Dozière, W. Dulinski, J.-C. Fontaine, M. Goffe, A. Himmi, Ch. Hu-Guo, K. Jaaskelainen, M. Koziel, F. Morel, C. Santos, M. Specht, I. Valin, G. Voutsinas, F.M. Wagner, M. Winter, “Improved radiation tolerance of MAPS using a depleted epitaxial layer,” *Nucl. Instr. and Meth. A*, vol. 624, pp. 432-436, Dec. 2010.
- A. Dorokhov, et al., “High resistivity CMOS pixel sensors and their application to the STAR PXL detector,” *Nucl. Instr. And Meth. A*, vol. 650, pp. 174-177, Sep. 2011.
- L. Greiner, E. Anderssen, H.S. Matis, H.G. Ritter, J. Schambach, J. Silber, T. Stezelberger, X. Sun, M. Szelezniak, J. Thomas, F. Videbaek, C. Vu, H. Wieman, “A MAPS based vertex detector for the STAR experiment at RHIC,” *Nucl. Instr. And Meth. A*, vol. 650, pp. 68-72, Sep. 2011.